Supramolecular Chemistry

DOI: 10.1002/anie.201200209

Solution-Phase Structures of Gallium-Containing Pyrogallol[4]arene Scaffolds**

Harshita Kumari, Steven R. Kline, Wei G. Wycoff, Rick L. Paul, Andrew V. Mossine, Carol A. Deakyne, and Jerry L. Atwood**

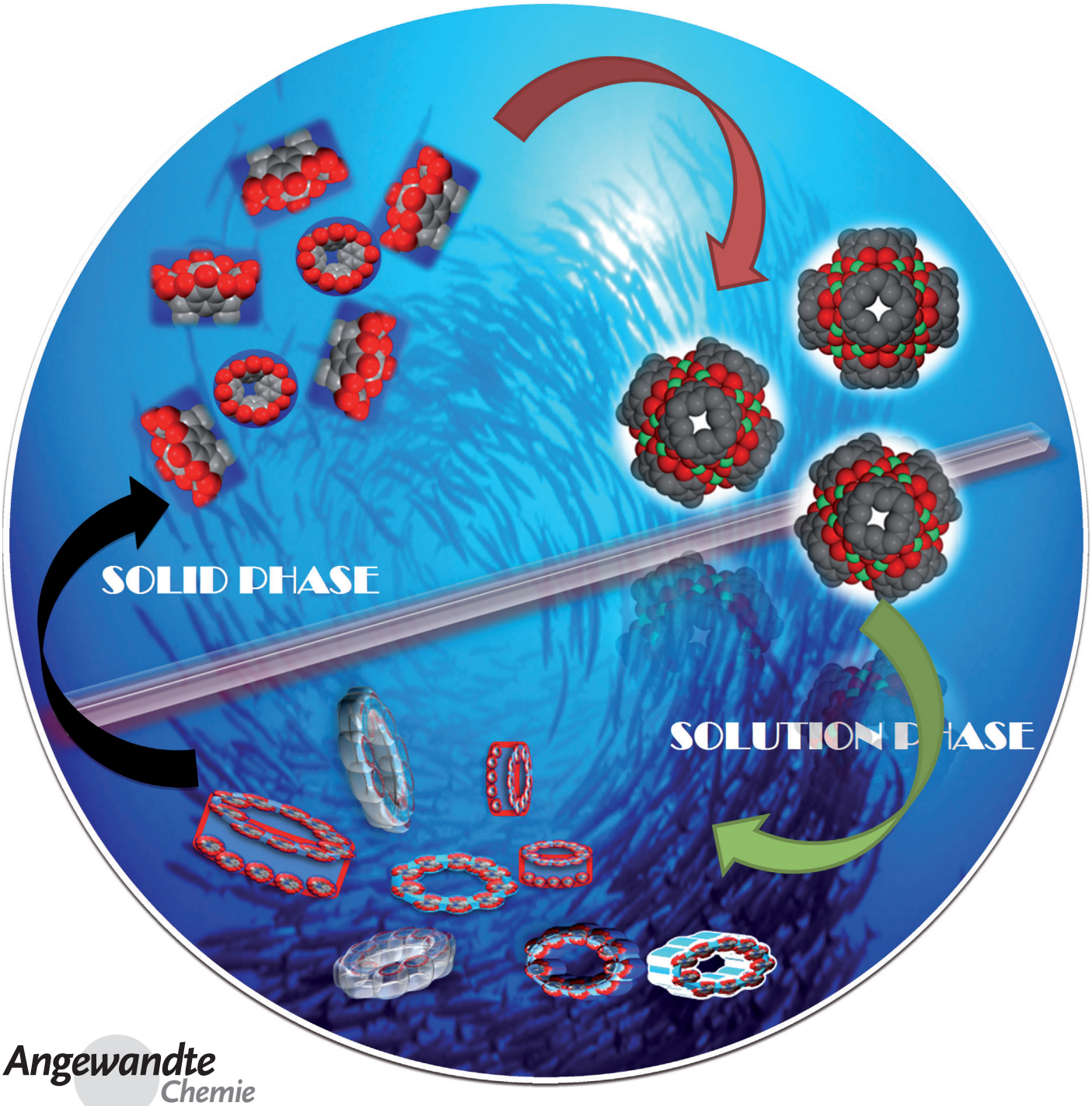

The synthesis of metal-seamed architectures continues to attract wide attention among supramolecular chemists. Understanding the properties of such metal-seamed systems could lead to practical applications such as biological probes,[1] electronic nanodevices,[2] or luminescent superparamagnetic hybrids.[3] Investigation of metal-seamed pyrogallol[4]arene organic nanocapsules (MONCs) dates back to 2005 with the formation of copper-seamed *C*-propan-3-ol-pyrogallol[4]arene hexamers.[4] In this assembly, six pyrogallol[4]arenes are partially deprotonated to yield a small rhombicuboctahedron with eight triangular [of $(O\text{-}Cu\text{-}O)_3$ units] and eighteen square faces. Later, zinc-seamed *C*-propylpyrogallol[4]arene (PgC_3Zn, where 3 is the alkyl chain length) dimeric nanocapsule was synthesized.[5]

Gallium is of particular interest with respect to MONCs, owing to its semiconducting properties and its ability to assemble into interesting architectures. For example, gallium cages,[6] gallium nanoparticles,[7] single-wall gallium nitride nanotubes,[8] and GaP nanowires, nanocables and nanobelts[9] have been reported. Amongst the pyrogallol[4]arene frameworks, gallium-containing scaffolds are unique in several aspects, such as the diversity of architectures, the metal to pyrogallol[4]arene ratio and the metal oxidation state.

Unlike the other observed dimeric and hexameric pyrogallol[4]arene nanocapsules, which are spherical, the gallium-seamed *C*-butylpyrogallol[4]arene (PgC_4Ga) hexamers have a distorted "rugby-ball" shape.[10] Compared to 24 copper atoms in a typical spherical hexamer, only 12 gallium atoms, along with four water molecules, seam this hexameric assembly. These gallium-seamed nanocapsules are particularly interesting owing to the Ga^{3+} ions occupying $Ga_3(\mu_3\text{-}O)_3(O)_6$ units on opposite planes seaming only four of the six PgC_4 moieties of the hexameric framework.[10] Water molecules seam the remaining two PgC_4 moieties, providing the first partially hydrogen-bonded metal-seamed hexamer. The gated aqueous channels can be utilized for ion transportation to the interior of the capsules.[11]

Gallium continued to show distinctive behavior when mixed-metal hexamers were synthesized.[11a] Addition of a second metal to a pre-formed gallium hexamer caused a transition in structure from the distorted rugby ball to a sphere (Figure 1). Subsequently, hexameric spheres of gallium–zinc, gallium–copper, gallium–nickel, and gallium–cobalt combinations were found.[11a] It was, however, difficult to distinguish between the metal atoms using single-crystal XRD because of the similar electronic densities of the metals involved. Hence, inductively coupled plasma (ICP) analyses were conducted to confirm the presence of the second metal and to obtain an approximate ratio of the metal ions in the framework.[11a]

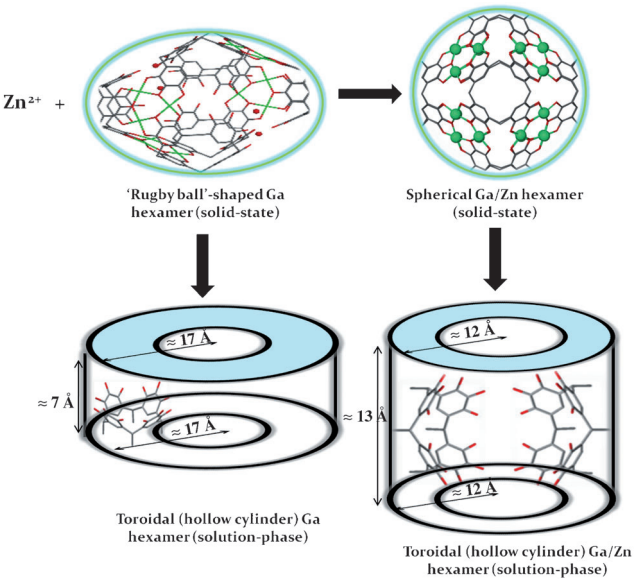

Figure 1. Geometries of gallium-seamed nanoassemblies as a function of addition of a second metal and change in phase.

Given the interesting solid-state properties of the gallium-based nanocapsules, we have investigated their geometric dimensions and shapes in solution with small-angle neutron scattering (SANS). We have also performed prompt gamma activation analysis (PGAA) of the solid-state capsules to support the earlier ICP results. To our knowledge, the only other solution-phase study of PgC_4Ga mixed-metal hexamers is a ^1H NMR study (CD_3CN) comparing the PgC_4GaZn hexamer to the PgC_4Ga hexamer.[12] The one definitive conclusion obtained from these studies was that solvent is encapsulated only in the presence of zinc. To obtain more specific structural details, we performed SANS measurements, 1-D NMR and 2-D HMQC and diffusion-ordered NMR spectroscopy for the PgC_4Ga and PgC_4GaZn nanoassemblies. Previously, we have employed SANS to examine the self-assembly process and geometric dimensions of the spherical PgC_3Cu and PgC_3Ni hexamers and dimers in solution.[13] These two sets of experiments will allow us to

[*] Dr. H. Kumari, Dr. W. G. Wycoff, A. V. Mossine, Prof. C. A. Deakyne, Prof. J. L. Atwood
Department of Chemistry, University of Missouri-Columbia
601 S. College Avenue, Columbia, MO 65211 (USA)
E-mail: deakynec@missouri.edu
atwoodj@missouri.edu
Dr. S. R. Kline
NIST Center for Neutron Research
National Institute of Standards and Technology
100 Bureau Drive, Gaithersburg, MD 20899 (USA)
Dr. R. L. Paul
Material Measurement Laboratory
National Institute of Standards and Technology
100 Bureau Drive, Gaithersburg, MD 20899 (USA)

[**] We thank NSF for support of this work (J.L.A.). This work utilized facilities supported in part by the National Science Foundation under Agreement No. DMR-0944772 (S.R.K.), NIBIB training grant T21 EB004822 (A.V.M.), NSF grant CHE-89-08304, NIH/NCRR S10 RR022341-01 (Cold probe) for NMR. Certain trade names and company products are identified to adequately specify the experimental procedure. In no case does such identification imply recommendation or endorsement by the National Institute of Standards and Technology, nor does it imply that the products are necessarily best for the purpose.

Supporting information for this article is available on the WWW under http://dx.doi.org/10.1002/anie.201200209.

identify any differences in the behaviour of a typical transition metal (copper/nickel)-seamed PgC*n* sphere and a gallium-seamed PgC*n* distorted rugby ball.

The PgC_4Ga hexameric crystals were formed by the earlier reported method of mixing acetone solubilized PgC_4 (0.26×10^{-3} mol L^{-1}) with water solubilized gallium nitrate (0.28 g in 2 mL water).[12] Likewise, the PgC_4GaZn hexamer crystals were obtained by adding a zinc nitrate ethanolic solution (0.28 g in 2 mL) to pre-formed and dried PgC_4Ga crystals that had been dissolved in acetone (0.015×10^{-3} mol L^{-1}).[12] A similar method was followed for the preparation of the Ga/Ni, Ga/Co, and Ga/Cu mixed-metal nanocapsules. Slow evaporation of each solution led to crystals suitable for structure elucidation. The unit cells for these crystals matched those obtained previously.[11a]

Cold neutron PGAA[14] was conducted to investigate the metal ratios in mixed-metal pyrogallol[4]arene frameworks and the results are compared with the earlier ICP analyses in Table 2. Interestingly, however, the new measurements lead to a noticeable trend in the metal ratios across the periodic table. The average mmol ratios of Ga^{3+}:M^{2+} decrease from approximately 2.8 for Ga^{3+}:Co^{2+} to 1.8 for Ga^{3+}:Ni^{2+} to 1.4 for Ga^{3+}:Cu^{2+} and to 1.3 for Ga^{3+}:Zn^{2+}. That is, as the atomic number of the transition metal increases, the transition metal fills more sites in the Ga/M hexameric framework, suggesting an enhanced affinity to stitch the hexameric framework from cobalt to zinc (Table 1).

Table 1: Metal ratios from prompt gamma activation analysis (PGAA) of Ga/M-seamed pyrogallol[4]arene hexamers.[a]

Metal 1:Metal 2	ICP analysis[b]	PGAA
Ga:Zn	14:10	13.5:10.5
Ga:Cu	13:11	14:10
Ga:Ni	15:9	15:9
Ga:Co	16:8	18:6

[a] Expanded uncertainties for PGAA values are estimated at $\leq 5\,\%$ based on counting statistics, background subtraction, purity of the standards, and neutron flux uncertainties. [b] Reference [10].

The SANS measurements were conducted on the NG7 30 m SANS instrument at the NIST Center for Neutron Research (NIST-NCNR) in Gaithersburg, MD.[15] Neutrons of wavelength $\lambda = 6$ Å with full width half-maximum $\Delta\lambda/\lambda = 15\,\%$ were used. Sample to detector distances of 1.3 m and 6 m were employed to cover the q range of $0.012\ \text{Å}^{-1} < q < 0.52\ \text{Å}^{-1}$, where q is the scattering vector. Pre-formed PgC_4Ga hexamers[11a] and PgC_4GaZn hexamers[11a] were dissolved separately in deuterated [D_6]acetone at a mass fraction of 2 %. Deuterated solvents improve the scattering contrast and thus the coherent scattering of neutrons that contains the structural information. The collected scattering data was then reduced and analyzed on software provided by NIST.[16] Factors such as instrumental geometry, apertures, wavelength spread, effect of gravity on neutron trajectory, etc. have been taken into account by employing resolution-smeared models for the data fitting and modeling. Smeared models provide a more accurate representation of the (smeared) experimentally measured scattering data.

The SANS data for typical PgC_3M hexamers and dimers fit to a polydisperse sphere,[17] with a radius of ca. 10 Å and ca. 7 Å, respectively.[13] These solution phase measurements correspond well with the previously reported XRD structures, which establishes the robustness of pyrogallol[4]arene-based MONCs in solution.[5,13,18] Given this parallel connection in shape and size in solution and solid phases, we expected the solution-phase scattering data for the PgC_4Ga and PgC_4GaZn nanoassemblies to fit to an ellipsoid and sphere, respectively. However, the fits to the uniform ellipsoid[19] and Schulz sphere[17a,20] models are of poor quality and indicate, for the first time, differences in the architectures of the nanoassemblies in the two phases (Supporting Information).

The PgC_4Ga and PgC_4GaZn neutron scattering data were then fitted to spherical polydisperse core–shell,[21] prolate core–shell,[17b,22] and hollow cylinder[19] models (see Supporting Information). The quality of the fit for the first two models is again very poor; the data fit exceptionally well, however, to the hollow cylinder model for both PgC_4GaZn and PgC_4Ga (Figures 1 and 2; Table 2). These are the first examples of cylindrical-shaped pyrogallol[4]arene nanoassemblies in solution. For this model, the scattering length densities (SLD) for the shell were calculated as $1.63\times10^{-6}\ \text{Å}^{-2}$ and $1.8\times10^{-6}\ \text{Å}^{-2}$ for PgC_4Ga and PgC_4GaZn, respectively. The solvent ([D_6]acetone) SLD was calculated as $5.39\times10^{-6}\ \text{Å}^{-2}$ and fixed to the hollow core.[19]

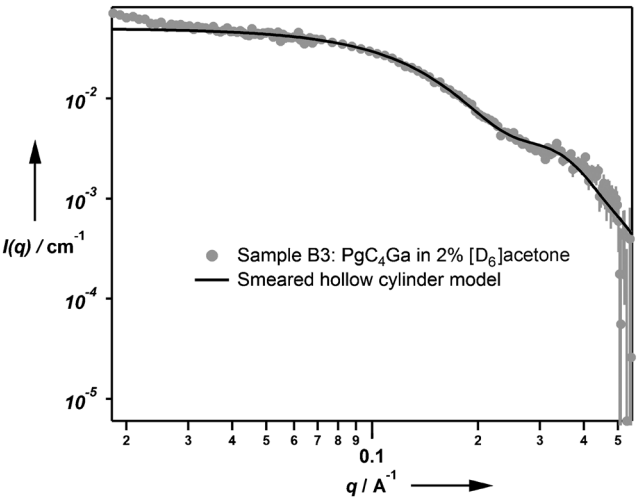

Figure 2. SANS data for the gallium-seamed *C*-butylpyrogallol[4]arene nanocapsule. A resolution-smeared hollow cylinder model is fitted to the SANS data (see text). Error bars on the SANS data represent one standard deviation.

Comparing the values from the fits, there is a minor variation in the core and shell sizes. The inner radius (core) increases by ca. 1.5 Å and the outer radius (shell) decreases by ca. 2 Å for PgC_4Ga compared to PgC_4GaZn. Overall, the shell thickness is about 4 Å larger for PgC_4Ga (12 Å) than for PgC_4GaZn (8 Å). In contrast, the length of the cylinder for PgC_4GaZn (13 Å) is twice that for PgC_4Ga (7 Å). Unexpectedly, the outer radius is larger than the length of the cylinder for both the PgC_4Ga and PgC_4GaZn species in solution. In fact, for the former species the shell diameter (34 Å) is more

Table 2: Resolution-smeared hollow cylinder fits to nanoassemblies of *C*-butylpyrogallol[4]arene gallium–zinc and gallium.[a]

Sample		Unit [Å][b]	SQRT [χ^2/N]
PgC_4GaZn	R_{core}	6.31 ± 0.15	1.070
	R_{shell}	14.52 ± 0.11	
	L	13.10 ± 0.24	
PgC_4Ga	R_{core}	4.78 ± 0.27	1.307
	R_{shell}	16.8 ± 0.17	
	L	6.9 ± 0.36	

[a] R_{core} = core radius; R_{shell} = shell radius; L = height. [b] Uncertainties in the fitted parameters are one standard deviation.

than four times the length of the cylinder, whereas for the latter species the shell diameter (29 Å) is more than twice the length of the cylinder (Table 2). The shape of the PgC_4Ga species in solution is thus a "donut-shaped/toroidal-shaped" assembly that expands in length on addition of the zinc metal ion. Similar self-assembled spherical and toroidal frameworks of dendrimersomes have been observed by Presec et al., reflecting the adaptibility of intermolecular interactions.[23]

It is important to note that Pg*Cn*s are not cylindrical in either the solid or solution phase. Hence, both the metal and solvent are playing a role in directing the solution-phase hollow cylindrical/toroidal architectures of the PgC_4Ga and PgC_4GaZn assemblies. It remains to be seen whether this interesting result will be observed for other gallium-based, mixed-metal species.

The variations in the structures of PgC_4Ga and PgC_4GaZn in the two phases suggest a conformational change in $[D_6]$acetone. To further study their solution-phase behavior and exhange dynamics, the PgC_4Ga and PgC_4GaZn nanoassemblies were investigated through ^1H, ^{13}C, ^{71}Ga, HMQC and diffusion-ordered (DOSY) NMR spectroscopy techniques. Because the peaks in the ^{13}C 1-D NMR spectra are too broad to be observed with sufficient signal-to-noise ratio, the ^{13}C peak positions for the linker and aromatic groups have been assigned through one-bond carbon–proton correlation in the HMQC (Supporting Information). HMQC indicates that the group of broad proton peaks between 6 and 8 ppm derive from protons directly bonded to the phenyl carbons (110 ppm) and that the peaks at 4.5 ppm derive from protons directly bonded to the linker carbons (35 ppm). The proton signals at 0.94 ppm and 1.4 ppm are correlated to the carbons of the CH_3 (14 ppm) and CH_2 (22 and 32 ppm) moieties, respectively, of the alkyl chains (Supporting Information). In addition to the peak broadening, the ^1H NMR spectra of PgC_4Ga and PgC_4GaZn show multiple peaks associated with the aromatic CH and linker CH protons, in contrast to the single ^1H signal from each of the two groups in PgC_4. PgC_4Ga and PgC_4GaZn show at least three environments for the aromatic CH group and two environments for the linker CH group. Note also the switch in the relative peak heights for the two sets of protons in the two toroidal nanoassemblies (Supporting Information).

Two peaks in the negative region (0 and −1.7 ppm) in the ^1H NMR spectra are observed only for PgC_4GaZn, suggesting that small molecules are encapsulated in only this toroidal nanoassembly. This result is consistent with that reported earlier for PgC_4Ga and PgC_4GaZn in CD_3CN.[12] The peak at 0 ppm produced a carbon counterpart (29 ppm) in the HMQC. This observation indicates that the encapulated molecule is either acetone or ethanol (some ethanol was present during sample preparation), but not water (Supporting Information).

PgC_4Ga has a diffusion coefficient in $[D_6]$acetone of $5.37 \times 10^{-10}\ m^2 s^{-1}$, which remains essentially unchanged even after 7 days ($5.33 \times 10^{-10}\ m^2 s^{-1}$). The corresponding diffusion coefficients for PgC_4GaZn and PgC_4 are $5.07 \times 10^{-10}\ m^2 s^{-1}$ and $8.65 \times 10^{-10}\ m^2 s^{-1}$, respectively. Furthermore, the diffusion coefficient for the entrapped small molecule is the same as that of the host PgC_4GaZn toroid. These diffusion coefficients are similar in magnitude to those found by Cohen and coworkers for hydrogen-bonded resorcin[4]arene and pyrogallol[4]arene hexamers in chloroform.[24]

The ^{71}Ga NMR spectra for the PgC_4Ga or PgC_4GaZn filtrate in $[D_6]$acetone shows a sharp peak from free gallium. In contrast, the ^{71}Ga NMR spectra for the crystalline hexamers dissolved in $[D_6]$acetone at both 27 °C and −70 °C reveals no recognizable signal, which indicates the absence of free gallium in solution (Figure 3). Overnight ^{71}Ga NMR spectroscopy on both PgC_4Ga and PgC_4GaZn in $[D_6]$acetone at room temperature produced no free gallium signal.

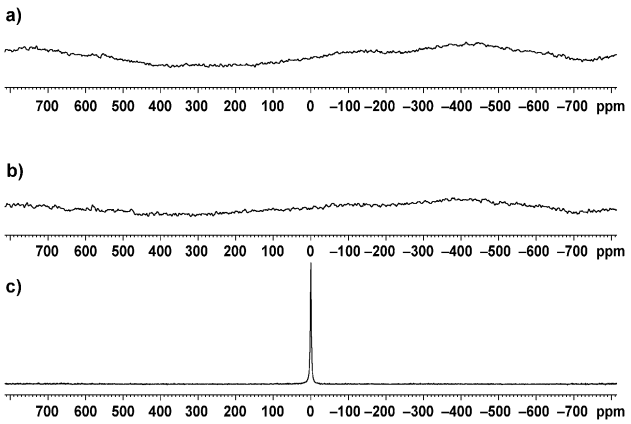

Figure 3. ^{71}Ga NMR spectra of a) PgC_4Ga crystals in $[D_6]$acetone at −70 °C and b) PgC_4Ga crystals in $[D_6]$acetone at 27 °C showing no signal for free gallium. c) Supernatant of PgC_4Ga at 27 °C showing a free gallium peak in $[D_6]$acetone. (The broad humps in the baseline in (a) and (b) are due to the probe's background.)

Overall, these experiments provide evidence for not only the presence of gallium in the self-assembled toroidal frameworks but also the stability of the frameworks. The experiments also demonstrate that the PgC_4GaZn toroids comprise solvent as well as metal and that the guest solvent remains encapsulated over time.

Combining the above SANS and NMR data and assuming the same metal content as observed from XRD and PGAA, we propose the following structural details for the solution-phase toroidal assemblies. Calulating the shell volume using Equation (1) yields a V_{shell} of 5600 $Å^3$ for the PgC_4Ga toroidal assembly and 7000 $Å^3$ for the PgC_4GaZn assembly.

$$V_{shell} = \pi(R_{shell}{}^2 - R_{core}{}^2)L \quad (1)$$

Both XRD and SANS measurements reveal the dimensions of ca. 14 × 7 Å for a typical PgC*n* (*n* = 1–4) bowl. The 7 Å length is the distance between the centroid of the linker carbons at the lower rim and the centroid of the oxygens at the upper rim. The 14 Å diameter is the distance between opposing oxygens at the upper rim. Thus, the difference of 1400 Å^3 in V_{shell} corresponds to the volume of 2 bowls of PgC_4. Assuming that the toroidal assemblies consist of only PgC_4 bowls, the individual shell volumes are consistent with 7 bowls in PgC_4Ga and 9 bowls in PgC_4GaZn.

The shorter axis of the PgC_4 bowl corresponds to the height of the PgC_4Ga toroid while the longer axis of the bowl corresponds to the height of the PgC_4GaZn toroid. This observation suggests a possible difference in the orientation of the PgC_4 macrocyles in the two toroidal assemblies, with the upper and lower rims of the macrocyles aligned with the upper and lower rims of the PgC_4Ga toroid but perpendicular to the upper and lower rims of the PgC_4GaZn toroid.

The suggested structure of the PgC_4Ga toroid has the 7 arenes in a boat conformation providing possible coordination sites for the 14 gallium ions between the flat pyrogallols on adjacent arenes and between opposite pyrogallols on the same arene. The sideways orientation of the 9 cone-shaped macrocyles in the PgC_4GaZn assembly allows guest encapsulation and provides sufficient coordination sites between adjacent arenes for the 24 metals that stitch the toroidal assembly (Figure 4). Among other possible interactions, the assemblies may also be stabilized by hydrogen-bonding between the pyrogallol hydroxy groups and solvent and by coordinate covalent bonds between the metal and solvent.

The proposed metal coordination sites lead to at least three different environments for the pyrogallol CH protons and two different environments for the linker group protons, as observed in the ^{1}H NMR spectrum. For example, focusing on the PgC_4Ga assemblies, because gallium interacts with only two of the three hydroxy groups of a given pyrogallol, all four of the aryl protons of a given arene are non-equivalent (Figure 4, bottom). The (at least) two different types of protons on the linker carbons arise for the same reason. If both gallium and zinc metals are present in the framework of the PgC_4GaZn assembly, as suggested by the difference in the toroidal dimensions, the more complicated multiple proton environments would be expected.

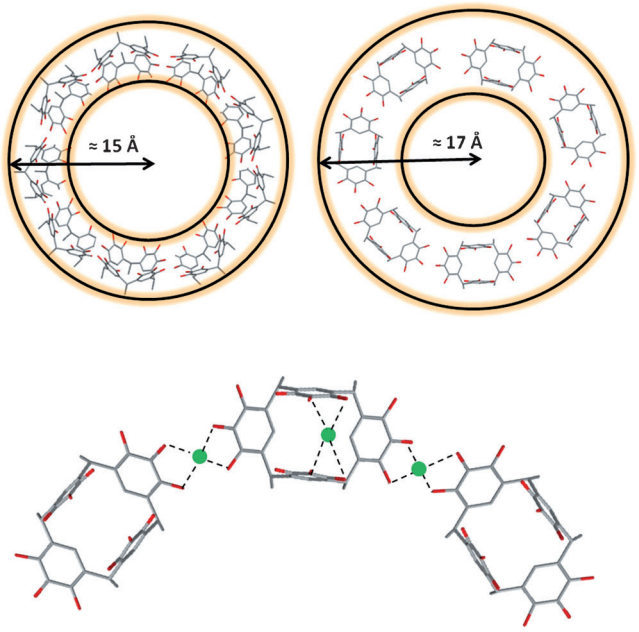

Figure 4. Top: Top view of the suggested arrangement of pyrogallol-[4]arenes in PgC_4GaZn (left) and PgC_4Ga (right) nanoassemblies in acetone. Bottom: Top view of the suggested metal coordination sites in the PgC_4Ga toroidal framework in acetone.

The results of the SANS, NMR and PGAA studies conducted in this work are intriguing because they demonstrate that PgC_4Ga nanoassemblies are distinctive in five ways: 1) the toroidal structure of the PgC_4Ga and PgC_4GaZn assemblies is different from the spherical structure of other PgC*n*M (M = Cu, *n* = 3–13; M = Ni, *n* = 3) assemblies[25] in the solution phase; 2) the rugby ball structure of the PgC_4Ga hexamer is different from the spherical structures of the PgC_3M (M = Cu, Ni) hexamers[13] in the solid state; 3) the structure of PgC_4Ga is different from that of PgC_4GaZn in the solid and solution phases; 4) guest encapsulation is not observed for the PgC_4Ga toroid in solution; 5) the Ga^{3+}:M^{2+} ratio in the PgC_4GaM hexamers varies with M, decreasing from Co^{2+} to Zn^{2+}. That is, the SANS measurements reveal the first structural change from the solid state to the solution phase, the NMR results reveal structural details unique to each toroid, and the PGAA measurements reveal the trend among the late 3d transition metals in directing the formation of mixed metal-seamed pyrogallol[4]arene nanoassemblies. Overall, the cohesive SANS and NMR experiments provide important insights into the solution-phase behavior of gallium-seamed *C*-butylpyrogallol[4]arene nanoassemblies.

Future studies will continue to address the ways in which non-covalent interactions and metal ions govern the self-assembly process of bi- and tri-metallic gallium-seamed nanoassemblies. In particular, combined solution-phase and computation studies will be performed to obtain more insight into the mechanism of formation of and metal ion positions in gallium-seamed scaffolds.

Received: January 10, 2012
Published online: April 18, 2012

Keywords: gallium · pyrogallol[4]arene · small-angle neutron scattering · supramolecular chemistry · toroids

[1] *Lanthanide Probes in Life, Chemical and Earth Sciences: Theory and Practice* (Eds.: J. C. G. Buenzli, G. R. Choppin), Elsevier, **1989**, p. 432.
[2] X. Cao, Y. Liang, *Mater. Lett.* **2009**, *63*, 2215–2217.
[3] C. W. Evans, C. L. Raston, K. S. Iyer, *Green Chem.* **2010**, *12*, 1175–1179.
[4] R. M. McKinlay, G. W. V. Cave, J. L. Atwood, *Proc. Natl. Acad. Sci. USA* **2005**, *102*, 5944–5948.
[5] N. P. Power, S. J. Dalgarno, J. L. Atwood, *New J. Chem.* **2007**, *31*, 17–20.
[6] a) J. S. Mugridge, R. G. Bergman, K. N. Raymond, *J. Am. Chem. Soc.* **2012**, *134*, 2057–2066; b) D. L. Caulder, R. E. Powers, T. N.

Parac, K. N. Raymond, *Angew. Chem.* **1998**, *110*, 1940 – 1943; *Angew. Chem. Int. Ed.* **1998**, *37*, 1840 – 1843.
[7] N. N. Kolesnikov, V. V. Kveder, D. N. Borisenko, E. B. Borisenko, A. V. Timonina, S. I. Bozhko, "Method of Gallium Nano-Particles Production Using Pulse Crystn.", 2336371, **2008**.
[8] J. W. Kang, H. J. Hwang, *Comput. Mater. Sci.* **2004**, *31*, 237 – 246.
[9] H. W. Seo, S. Y. Bae, J. Park, *Mater. Res. Soc. Symp. Proc.* **2004**, *789*, 285 – 290.
[10] R. M. McKinlay, P. K. Thallapally, G. W. V. Cave, J. L. Atwood, *Angew. Chem.* **2005**, *117*, 5879 – 5882; *Angew. Chem. Int. Ed.* **2005**, *44*, 5733 – 5736.
[11] a) P. Jin, S. J. Dalgarno, J. L. Atwood, *Coord. Chem. Rev.* **2010**, *254*, 1760 – 1768; b) S. J. Dalgarno, N. P. Power, J. L. Atwood, *Coord. Chem. Rev.* **2008**, *252*, 825 – 841.
[12] "Synthesis of Mixed Metal – organic Pyrogallol[4]arene Nanocapsules and their Host – guest Chemistry": P. Jin, Ph.D. Thesis, University of Missouri-Columbia, **2009**.
[13] H. Kumari, A. V. Mossine, S. R. Kline, C. L. Dennis, D. A. Fowler, C. L. Barnes, S. J. Teat, C. A. Deakyne, J. L. Atwood, *Angew. Chem.* **2012**, *124*, 1481 – 1483; *Angew. Chem. Int. Ed.* **2012**, *51*, 1452 – 1454.
[14] R. L. Paul, R. M. Lindstrom, A. E. Heald, *J. Radioanal. Nucl. Chem.* **1997**, *215*, 63 – 68.
[15] C. J. Glinka, J. G. Barker, B. Hammouda, S. Krueger, J. J. Moyer, W. J. Orts, *J. Appl. Crystallogr.* **1998**, *31*, 430 – 445.
[16] S. R. Kline, *J. Appl. Crystallogr.* **2006**, *39*, 895 – 900.
[17] a) G. V. Schulz, *Z. Phys. Chem.* **1939**, *B43*, 25 – 46; b) M. Kotlarchyk, S. H. Chen, *J. Chem. Phys.* **1983**, *79*, 2461 – 2469.
[18] J. L. Atwood, E. K. Brechin, S. J. Dalgarno, R. Inglis, L. F. Jones, A. Mossine, M. J. Paterson, N. P. Power, S. J. Teat, *Chem. Commun.* **2010**, *46*, 3484 – 3486.
[19] D. I. Svergun, L. A. Feigin, *X-ray and Neutron Low-Angle Scattering*, **1986**, p. 278.
[20] G. V. Schulz, *Z. Phys. Chem.* **1935**, *B30*, 379 – 398.
[21] P. Bartlett, R. H. Ottewill, *J. Chem. Phys.* **1992**, *96*, 3306 – 3318.
[22] S. S. Berr, *J. Phys. Chem.* **1987**, *91*, 4760 – 4765.
[23] V. Percec, D. A. Wilson, P. Leowanawat, C. J. Wilson, A. D. Hughes, M. S. Kaucher, D. A. Hammer, D. H. Levine, A. J. Kim, F. S. Bates, K. P. Davis, T. P. Lodge, M. L. Klein, R. H. DeVane, E. Aqad, B. M. Rosen, A. O. Argintaru, M. J. Sienkowska, K. Rissanen, S. Nummelin, J. Ropponen, *Science* **2010**, *328*, 1009 – 1014.
[24] a) L. Avram, Y. Cohen, *J. Am. Chem. Soc.* **2002**, *124*, 15148 – 15149; b) L. Avram, Y. Cohen, *Org. Lett.* **2003**, *5*, 3329 – 3332.
[25] a) H. Kumari, S. R. Kline, N. J. Schuster, J. L. Atwood, *Chem. Commun.* **2011**, *47*, 12298; b) H. Kumari, S. R. Kline, N. J. Schuster, C. L. Barnes, J. L. Atwood, *J. Am. Chem. Soc.* **2011**, *133*, 18102 – 18105.

